International Journal of Environmental Science and Technology
https://doi.org/10.1007/s13762-021-03711-6

ORIGINAL PAPER

Synthesis, characterization, and textile dye adsorption studies of a kaolin-based polymer layer silicate composite

R. E. A. Dissanayake[1] · I. M. Premarathne[2] · S. S. Iqbal[3] · N. Priyantha[4] · M. C. M. Iqbal[1]

Received: 4 June 2021 / Revised: 4 September 2021 / Accepted: 27 September 2021

Abstract

Contamination and exposure to textile dye wastewater are environmental issues of grave concern, especially in developing countries. The use of advanced technologies to remediate wastewater is not economical for small- and medium-sized industries. An environmentally friendly and economical method was developed to adsorb dyes from wastewater using a composite material, prepared by the sol–gel method. The surface area was 18.16 m^2/g and the pH at the point of zero charge (pH_{PZC}) was 4.2. The peak shifts in Fourier transform infrared spectra upon adsorption indicated the functional groups involved in adsorption while scanning electron microscopic images indicated that exfoliated and intercalated polymer layer silicate structures are present in the composite. The composite dose of 0.20 g adsorbed over 90% of fuchsine and methylene blue dyes after 240 min and 330 min, respectively. The experimental data of fuchsine adsorption agreed with the Langmuir–Freundlich combined isotherm while methylene blue adsorption data obeyed the Freundlich isotherm alone. Fuchsine dye forms Hydrogen (H)-bonds and H–π interactions with the adsorbent surface, and H-bonds and π–π interactions between the dye molecules to form multilayers. The methylene blue forms H–π interactions with the adsorbent surface. The composite can remove negatively charged dyes since the adsorption surface is positively charged even at pH 7. The composite dose of 0.20 g reduced the absorbance of dyes in wastewater within 6 h of agitation. This shows that the adsorbent has the potential to remove pigment dyes and direct dyes present in industrial wastewater.

Editorial responsibility: Parveen Fatemeh Rupani.

✉ M. C. M. Iqbal
iqbal.mo@nifs.ac.lk

[1] Plant and Environmental Sciences Laboratory, National Institute of Fundamental Studies, Kandy, Sri Lanka

[2] Instrument Center, University of Sri Jayewardenepura, Nugegoda, Sri Lanka

[3] Department of Chemistry, Faculty of Natural Sciences, Open University of Sri Lanka, Nugegoda, Sri Lanka

[4] Department of Chemistry, Faculty of Science, University of Peradeniya, Kandy, Sri Lanka

Graphic Abstract

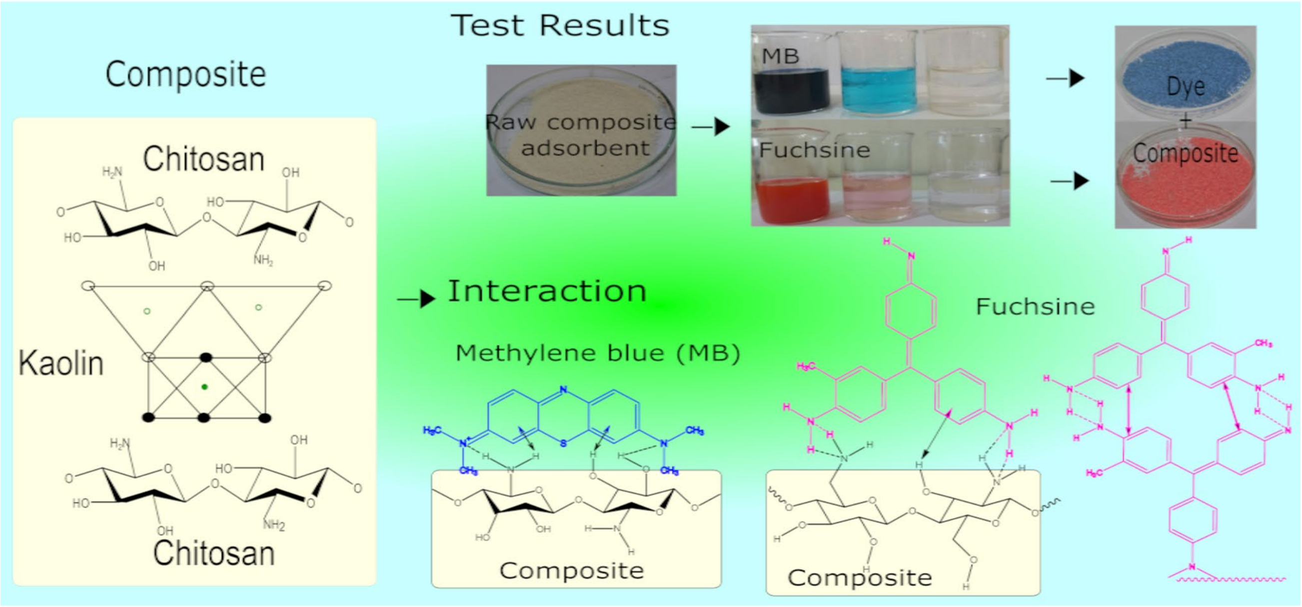

Keywords Adsorption · Chitosan · Kaolin · Polymer layer silicate composites · Textile dyes

Introduction

The absence of good environmental practices has created many health hazards, particularly in developing countries. Among them, textile dye contamination of waterways, which feed into drinking and irrigation water, is a major environmental health hazard (Chequer et al. 2013). For small- and medium-scale enterprises (SME), investing in expensive decontamination methods is uneconomical. They invariably discharge effluents with organic dyes into waterways. This is a serious environmental hazard since organic dyes are toxic to aquatic life, and further, their biodegradability is low (Monvisade and Siriphannon 2009; Nesic et al. 2012). Even though advanced decontamination methods are available, most of them are expensive and technically demanding for implementation by small-scale entrepreneurs, who need to be incentivized to adopt these methods. Further, physicochemical methods commonly used for wastewater decontamination are expensive and invariably produce toxic sludge (Rosales et al. 2017). On the other hand, biological methods are a cost-effective alternative; but the adverse effects of wastewater, such as toxicity, acidity, and light penetrability in aqueous systems, limit their application. Consequently, development of cost-effective and efficient green adsorbent materials for the removal of textile dyes from wastewater is imperative (Rosales et al. 2017). In this context, dye removal using solid adsorbents is a promising technique to remove organic dyes since it is simple, insensitive to toxic environments, cost efficient, and easy to operate (Karaca et al. 2008; Zhu et al. 2010).

Polymers can be broadly classified as biobased (e.g., chitin, chitosan, keratin, starch, etc.), and synthetic polymers (e.g., polyethylene, polypropylene, polyethylene terephthalate, etc.) (Jiang and Zhang 2017; Asgher et al. 2020). Of these, biobased polymers are non-toxic, biodegradable, economical, and environmentally friendly (Iqbal et al. 2018). Polymer layer silicate (PLS) composites are a new class of material (Alexandre and Dubois 2000) that has attracted attention in the fields of automotive, construction, aerospace, food packaging, and textile industries due to their performance, mechanical properties, and cost-effectiveness (Paul and Robeson 2008; Pavlidou and Papaspyrides 2008; Mittal 2009). Although a few studies have reported their use in adsorption (Xie et al. 2011; Wan Ngah et al. 2011), PLS composites have not been investigated as adsorbents for wastewater treatment.

In this context, a low-cost PLS composite adsorbent was developed using chitosan and kaolin. Since chitosan is a waste product from aquaculture and kaolin is naturally abundant, only acetic acid and NaOH are required for the synthesis of the composite; its production is relatively low-cost compared to expensive chemicals used for effluent treatment. Clay minerals in their natural and modified forms have been used for many years as effective adsorbents (Amer et al. 2010; Meroufel et al. 2013). However, the use of clay minerals in water treatment is a challenge since the clay disintegrates and renders the water turbid. Kaolinite clay, an adsorbent in its raw form, increases the turbidity of the water, which requires fine filters for removal.

In this study, a composite material was developed using kaolinite clay and chitosan, a biopolymer derived from chitin extracted from waste products such as crab shells, shrimp shells, and fish scales (Islam et al. 2011; Mota et al. 2012). It is a natural biopolymer suited for immobilization because of its hydrophilicity, biodegradability, nontoxicity, and availability (Cestari et al. 2008; Wan Ngah et al. 2011). Chitosan is able to capture anionic dyes due to electrostatic attraction between the protonated amine groups on the chitosan and the sulfonic groups of the anionic dyes which is beneficial to increase adsorption with the immobilized adsorbent (Chang and Juang 2004; Zhou et al. 2011; Zhu et al. 2011). Composites of chitosan have excellent biosorbent properties, such as cationic and macromolecular structure with a high capacity for adsorption (Vakili et al. 2014; Qamar et al. 2020). Physical and mechanical properties of chitosan can be further improved for dye adsorption using a crosslinker to form an intermolecular bridge between the macromolecules of chitosan (Qamar et al. 2020). Therefore, a combination of both materials is expected to produce a PLS composite with enhanced mechanical strength and adsorption capacity for anionic dyes.

This research paper describes the synthesis of a composite adsorbent from chitosan and kaolin to remove fuchsine and methylene blue dyes from aqueous environments. Experiments were conducted under controlled laboratory conditions with varying pH of the medium, contact time, and initial dye concentration, to simulate actual environmental settings. The dyes selected represent typical cationic dyes used in the textile industry and are good candidates for the study of adsorption by composites. Different kinetics and isotherm models were used to investigate the mechanism of the adsorption process. The efficiency of the composite adsorbent to remove dye waste from industrial wastewater was also determined.

The work reported herein was carried out at the National Institute of Fundamental Studies (NIFS), Kandy, Sri Lanka during 2017–2019.

Materials and methods

Instrumentation

Analytical-grade chemicals were used from BDH Chemicals, UK, Sisco Research Laboratories (Pvt.) Ltd. Mumbai, India, and Sigma-Aldrich Chemicals, St. Louis, MI, USA. Concentrations of fuchsine ($C_{20}H_{19}N_3 \cdot HCl$) and methylene blue ($C_{16}H_{18}ClN_3S$) were determined using a UV–visible spectrophotometer (Analytik Jena Specord 210 Plus, Jena, Germany) at their characteristic wavelengths of 543 nm and 668 nm, respectively. Hatch Hd 30Q portable pH meter was used to measure the pH of the dye solutions. FTIR spectra of samples before and after dye adsorption were recorded in the wavenumber range, 4000–400 cm^{-1} using FTIR spectrophotometer (Bruker, Ettlingen, Germany). Dye wastewater was characterized using a multiparameter analyzer to determine pH and conductivity (EUTECH Instruments, Pioneer, Singapore).

Preparation of the adsorbent

Kaolin was collected from a local mining site near Galaha, Sri Lanka. Thoroughly cleaned kaolin samples were air-dried and thereafter oven-dried at 105 °C for 2 days. To prepare the composite, 2.0 g of dry chitosan powder (Sigma Aldrich Chemicals, St. Louis, MI, USA) was dissolved in 150 mL of 1% acetic acid (Sigma Aldrich Chemicals, St. Louis, MI, USA) and the suspension stirred for 24 h. Thereafter, 40.0 g of dry kaolin was added to the chitosan solution and the mixture stirred for 24 h. The kaolin–chitosan mixture was then added to 0.5 mol/L NaOH solution dropwise to form beads. Resulting kaolin–chitosan beads were kept for 48 h, and excess NaOH was removed. The adsorbent material was washed with distilled water until the solution was neutral. Finally, the composite material was dried at 60 °C for 3 days, ground and sieved to obtain particles between 250 and 350 μm size (Kalemtas 2019).

Characterization of the adsorbent

Surface characterization

The surface of the adsorbent was characterized using the methylene blue adsorption method to determine surface area of the adsorbent (Chathuranga et al. 2014). Subsequently, the surface charge density of the adsorbent was determined by potentiometric auto titration (Metrohm 848 Titrino plus, Herisau, Switzerland) against a $NaNO_3$ solution (0.001–0.1 mol/L) (Fein et al. 2005; Dissanayake et al. 2016). An FTIR spectral analysis was performed before and after the adsorption of dye to determine the surface functional groups (Dissanayake et al. 2016). The surface morphology of the adsorbent was determined using a scanning electron microscope (Zeiss Evo LS15, Jena, Germany).

Effect of experimental parameters on adsorption

The effect of contact time on dye adsorption was investigated by shaking 0.2 g of dried composite material with 5.0 mg/L dye solution (100 mL) in an orbital shaker at 100 rpm. Suspensions were removed at desired time intervals and filtered, and the filtrate analyzed using UV–visible spectrophotometer. To study the effect of pH on adsorption, 0.2 g of the adsorbent was shaken with the dye solution at different pH values within 1–10. Different initial dye concentrations (1.0 mg/L to 30.0 mg/L) were used to determine the effect of initial dye concentration on dye removal. After equilibrium, suspensions were removed from the shaker and filtered. The filtrate was analyzed using UV–visible spectrophotometry.

Since ambient temperature conditions provided reasonably high extent of adsorption on kaolin–chitosan composite, higher temperatures were not attempted.

Treatment of industrial dye waste

Industrial wastewater samples were provided by a textile manufacturing factory in Kelaniya, Sri Lanka. The pH and conductivity of the dye wastewater samples were measured before and after treatment using a Multiparameter instrument. The wavelengths at maximum absorption were determined from the UV–visible spectra of wastewater samples containing direct dye and pigment dye for adsorption studies. Each dye sample was shaken with 0.2 g of kaolin–chitosan adsorbent for 6.0 h (360 min), and the suspension was removed and filtered. The filtrate was analyzed for the residual dye by scanning the residual solution using UV–visible spectrophotometry in the wavelength range 190–1100 nm.

Results and discussion

Results

Surface characterization

Surface area and the surface charge density of the adsorbent

To determine the surface charge density of the adsorbent, we used the following equation described in reference (Dissanayake et al. 2016).

$$\sigma = \{[F/(a \times s)]\}\{(C_a - C_b) - [\mathrm{H}^+] + [\mathrm{OH}^-]\} \quad (1)$$

where F and a denotes the Faraday constant, and the mass of the adsorbent in the suspension (1.00 g), respectively; C_a and C_b denotes the acid and base concentrations (mol L^{-1}), respectively; $[H^+]$ and $[OH^-]$ denotes the hydrogen and hydroxyl ion concentrations in the medium according to re-measured pH value at a particular point (Dissanayake et al. 2016).

The average number of methylene blue molecules adsorbed onto the composite surface was 1.16×10^{-7} mol; from this the surface area was (s) determined to be 18.16 m^2/g.

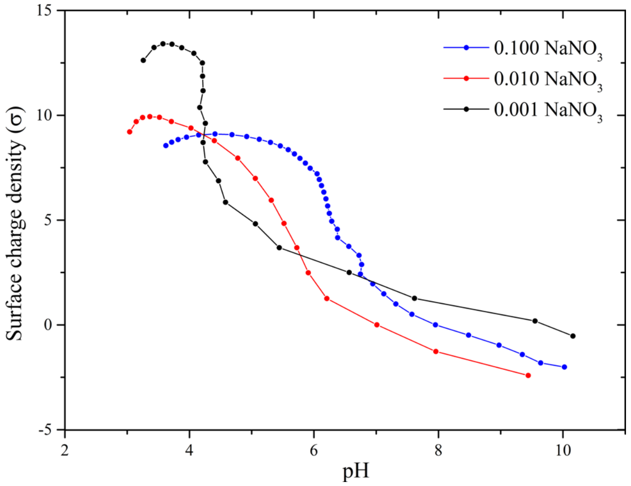

Fig. 1 Surface charge density variation of the adsorbent with external pH at three different ionic strengths: 0.001 mol/L $NaNO_3$ (——), 0.010 mol/L $NaNO_3$ (——), 0.100 mol/L $NaNO_3$ (——)

Figure 1 shows that the surface charge of the adsorbent changes with pH and the ionic strength of the solution. The surface was positively charged at lower pH values ($pH < 7$) and negatively charged at $pH > 7$ for ionic strengths between 0.1 M and 0.001 M solutions. The isoelectric point was at pH 4. At acidic pH ($pH < 7$), most of the functional groups would be protonated. Kaolin contains silicate (Si–O–) and aluminate (Al–O–) (Saikia and Parthasarathy 2010), and chitosan contains hydroxyl (–OH) and amine ($-NH_2$) groups (Rekik et al. 2017), some of which can be protonated to Si–OH, Al–OH, and $-NH_3^+$ when the H^+ concentration in the solution is increased. This can be the reason for the positively charged surface of the kaolin–chitosan composite in acidic medium. More importantly, the pH at the point of intersection of the three graphs, which is 4.2, can be taken as the pH at the point of zero charge.

Surface morphology of the adsorbent

FTIR spectra of kaolin–chitosan composite shows several adsorption sites (functional groups) present on the surface (Fig. 2). Among them, hydroxyl groups of kaolin (Si–OH, 3698 cm^{-1}, 3621 cm^{-1}) [32,33], bonded hydroxyl groups (–OH, 3471 cm^{-1}) [34], alkyl amine group ($R-NH_2$, 1637 cm^{-1}, 1618 cm^{-1}), Si–OH bond at 1116 cm^{-1}, at 1034 cm^{-1} the alcohol groups (C–OH), and in-plane Si–O at 1007 cm^{-1} (Tironi et al. 2012; Mgbemena et al. 2013) are notable.

Fig. 2 FT–IR spectrum of kaolin–chitosan composite adsorbent; before adsorption (——), after fuchsine adsorption (——), and after methylene blue adsorption (——)

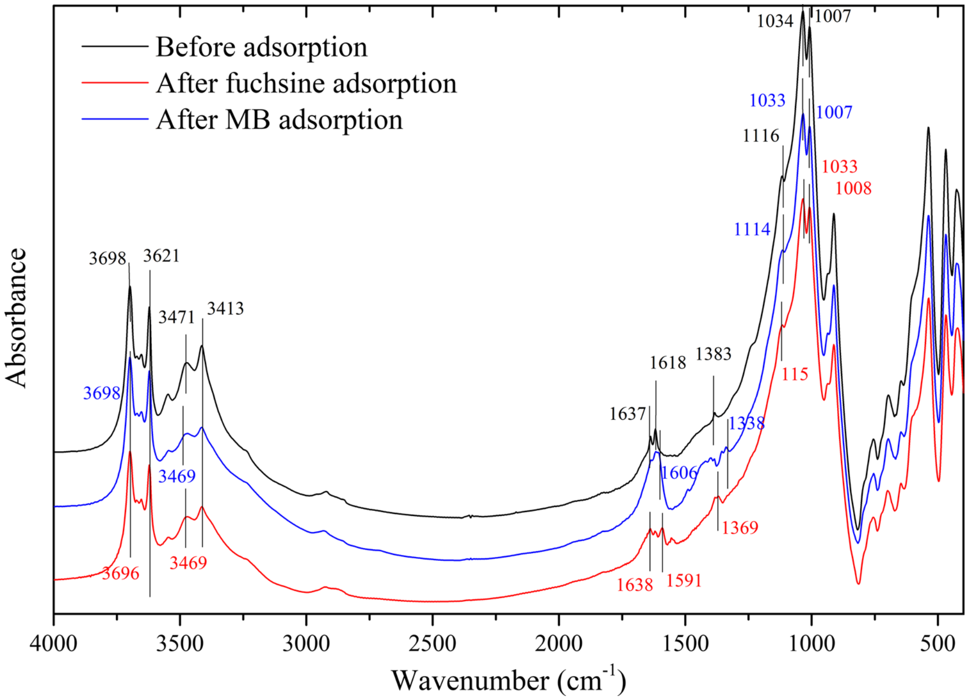

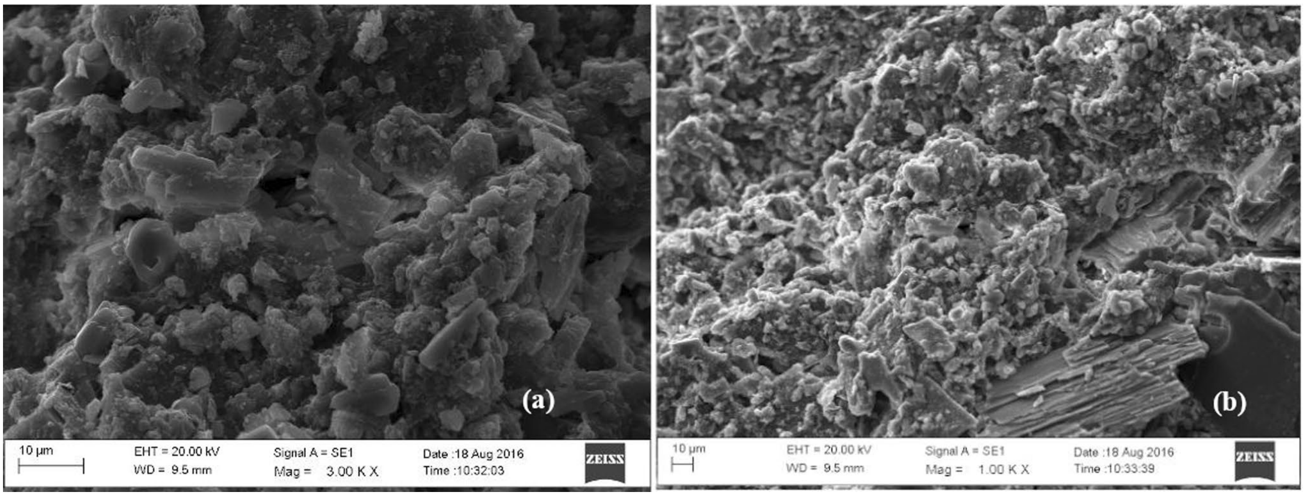

Fig. 3 Scanning electron microscopic images of (**a**) exfoliated and (**b**) intercalated composite structures

After fuchsine adsorption, the peak positions corresponding to the inner surface hydroxyl groups of kaolin, bonded hydroxyl groups, and alkyl amide group have shifted to 3696 cm^{-1}, 3469 cm^{-1}, 1591 cm^{-1}, and 1369 cm^{-1}, respectively. This indicates the involvement of the above functional groups in fuchsine dye adsorption. Similarly, peak positions shifted corresponding to bonded hydroxyl groups, and alkyl amine shifted to 3469, 1696, and 1338 cm^{-1} after methylene blue adsorption, which indicate their involvement in methylene blue adsorption.

It is evident from scanning electron microscopic images that the surface of the adsorbent is rough (Fig. 3). It also shows that there are two main configurations of exfoliated (Fig. 3a) and intercalated (Fig. 3b) polymer layer silicate structures present in the composite.

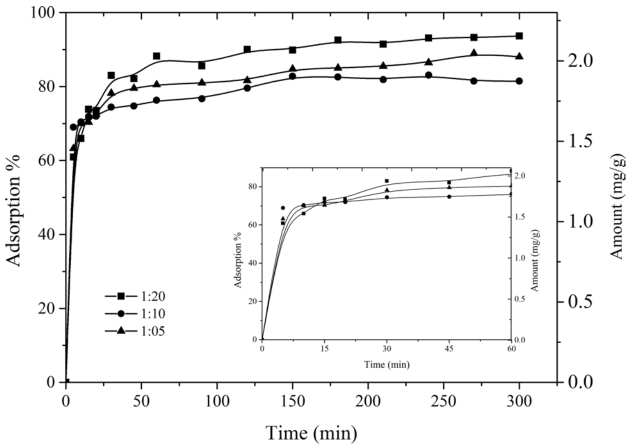

Fig. 4 Effect of the ratio of kaolin:chitosan ratio on fuchsine dye adsorption by the composite ($C_i = 5.0$ mg/L, adsorbent dose = 0.2 g, pH = 5.0, $T = 27$ °C, shaking speed 100 rpm, $n = 3$, 5:1 = —▲—, 10:1 = —●—, 20:1 = —■—)

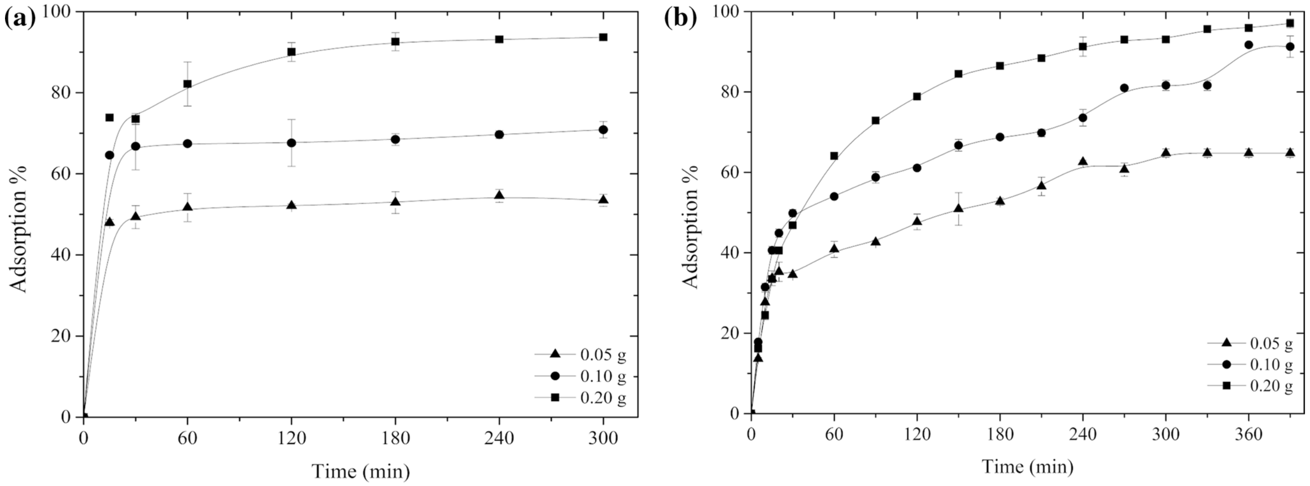

Fig. 5 **a**: Effect of contact time on the adsorption of fuchsine onto the kaolin–chitosan composite. **b**: Effect of contact time on the adsorption of methylene blue on to the kaolin–chitosan composite ($C_i = 5.0$ mg/L, adsorbent dose = 0.2 g, pH = 5.0, $T = 27$ °C, shaking speed 100 rpm, $n = 3$, 0.05 g = —▲—, 0.10 g = —●—, 0.20 g = —■—)

Effect of experimental parameters

Selection of Kaolin–Chitosan ratio for adsorption

The effect of contact time on percentage adsorption of dye on the composite was studied for kaolin–chitosan ratios of 5:1, 10:1, and 20:1 to select the most suitable ratio for dye adsorption. The percentage adsorption of fuchsine dye on the composite increased with increasing kaolin–chitosan ratio, with no appreciable change from the kaolin–chitosan ratio from 5:1 to 10:1 (Fig. 4). The maximum adsorption was shown for 20:1 ratio.

The ratio of the amount of kaolin to that of chitosan determines the number of functional groups in the composite adsorbent. Generally, when the amount of chitosan in the composite is increased, the surface activity of functional groups in the adsorbent also increases, thus enhancing the adsorption capacity. However, the maximum adsorption percentage of 93% was at a kaolin:chitosan (K:C) ratio of 20:1 and there was no appreciable change in percentage adsorption from K:C of 5:1 (83%) to 10:1 (81%) (Fig. 4). This indicates that the increase in K:C ratio from 5:1 to 10:1 has not appreciably altered the activity of surface functional groups leaving the adsorption capacity relatively unaffected. At a K:C ratio of 5:1, the adsorption percentage increased due to the availability of more functional groups. The number of functional groups is less in the composite whose K:C ratio is 10:1, and hence the adsorption capacity was low. In a 20:1 composite there are voids and deformations on the adsorbent surface, which may increase the surface area of the adsorbent, thereby increasing the adsorption capacity. The further increase in kaolin-to-chitosan ratio results in an unstable adsorbent; therefore, 20:1 ratio was selected as the optimum kaolin:chitosan ratio for the composite.

Effect of contact time on the adsorption process

Contact time is a key parameter in determining the efficiency of a particular adsorbent. In this study, the extent of dye adsorption increased with increasing contact time, reaching a constant value for all the composite doses. The extent of adsorption increased with increasing dose of the composite, with the maximum adsorption of 93% (2.13 mg/g), which was achieved after 240 min for the adsorption of fuchsine at the composite dose of 0.20 g (Fig. 5a).

However, for methylene blue, adsorption reached equilibrium after 330 min, and the amount of dye adsorbed was 95% for the composite dose of 0.20 g (Fig. 5b). The highest extent of adsorption at the lower adsorbent dose of 0.05 g was 54% and 64% for fuchsine and methylene blue, respectively. Since the optimum time for equilibrium did not depend on the adsorbent amount, 240 min and 330 min were selected as the optimum shaking times for fuchsine and methylene blue, respectively.

The number of adsorption sites on the adsorbent surface determines the adsorption percentage; an adsorbent surface with a higher number of adsorption sites is expected to show a higher adsorption percentage. The extent of adsorption is determined by the availability of the adsorption sites on the adsorbent surface, while the rate of adsorption depends on diffusion characteristics and the strength of attraction. Even though the same adsorbent was employed in this study, methylene blue was not adsorbed as rapidly as fuchsine. Within the first 15 min of the adsorption process, 73% of fuchsine was absorbed in contrast to the corresponding value of 33% for methylene blue. The different rates of initial adsorption of the two dyes by the same adsorbent may be due to the different chemical nature of the two adsorbates. The fuchsine molecule has three functional amine groups; these amine groups easily form interactions with the functional groups of the adsorbent. In contrast, methylene blue has two accessible $–N(CH_3)_2$ functional groups and a 1,4-thiazine unit. Thus, the interactions are not strong enough to attach the methylene blue dye molecule onto the adsorbent surface, which can be released back into the bulk solution upon reaching equilibrium. The concentration gradient between the fuchsine dye on the adsorbent surface and the bulk solution is high, and hence, a rapid adsorption of dye molecules was observed (Guo et al. 2003; Dissanayake et al. 2016). On the other hand, methylene blue maintained a slow and steady adsorption rate. The interactions during the dye adsorption are mainly (1) exchange of electrons between the dye and the adsorption sites, which is a slow process; (2) hydrogen bond formation between the adsorbent surface and the dye; and (3) charge interactions between the adsorbent surface and the π electron cloud of the benzene rings of the dye, which are physisorption (Volesky 2003).

Effect of pH on the adsorption process

The initial pH of the dye solution affects the adsorption capacity and the stability of the adsorbent. It was found that the adsorbent is not stable when the solution pH is below 3. The surface charge variation with the solution pH shows that the adsorbent is positive when the surrounding pH is below 7 (Fig. 1). This is due to the protonation of the surface amine groups to form $–CH_2–NH_3^+$.

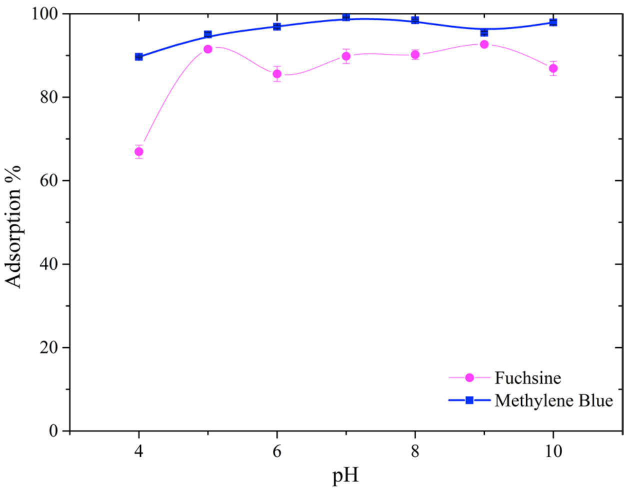

Fig. 6 Effect of initial pH on the adsorption of fuchsine (●) and methylene blue (■) onto 0.20 g of kaolin–chitosan composite material ($C_i = 5.0$ mg/L, adsorbent dose = 0.2 g, $T = 27$ °C, shaking speed 100 rpm, $n = 3$,)

In solutions of low pH, amine groups of the fuchsine molecule can be protonated to form positively charged $–CH_2–NH_3^+$ and $C=NH_2^+$. Methylene blue molecule contains –N=, –S–, $–N–(CH_3)_2$ groups, which can also be protonated at low pH. These positively charged functional groups and positively charged adsorbent surfaces repel each other. However, the protons present in the $–CH_2–NH_3^+$ groups can easily form interactions with the π electron cloud of the benzene group in the dye molecules. This results in a moderate adsorption (66%) of fuchsine at pH 4.0, and 89% of methylene blue adsorption. In the pH range between 5.0 and 9.0, maximum adsorption percentages of 93% and 95% were observed for fuchsine and methylene blue, respectively (Fig. 6). Therefore, the optimum pH for adsorption is between pH 5.0 and 9.0. The ambient pH of both dye solutions is pH 5.0, and therefore, pH 5.0 was selected as the optimum pH for further experiments.

These observations confirm the results of previous studies on the adsorption of cationic dyes on different adsorbents, such as fuchsine adsorption on bottom ash and deoiled soya (Gupta et al. 2008), and methylene blue on wheat shells (Bulut and Aydın 2006).

Effect of shaking speed on the adsorption process

The required macroscopic exchange of adsorbate and adsorbent is provided by shaking the adsorption system. The mixing of the adsorbent and the adsorbate should be optimum since slow mixing rates will result in a low

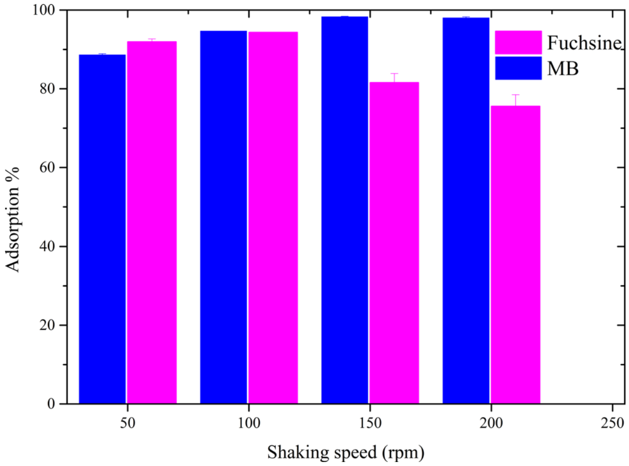

Fig. 7 Effect of shaking speed on fuchsine (🟪) and methylene blue (🟦) adsorption onto kaolin–chitosan composite adsorbent ($C_i = 5.0$ mg/L, adsorbent dose = 0.2 g, pH = 5.0, $T = 27$ °C, $n = 3$,)

adsorption percentage. At high mixing rates, low adsorption percentage will be observed due to the lower resident time of adsorbent and adsorbate. The percentage adsorption of methylene blue increased from 88 to 98% with increasing shaking speed from 50 to 150 rpm and remained the same thereafter. However, for fuchsine, percentage adsorption initially increased slightly from 91 to 93% (Fig. 7) when the shaking speed increased from 50 to 100 rpm, and then decreased to 75% with further increase in shaking speed to 200 rpm. Therefore, the shaking speed of 100 rpm was selected for all the other experiments with both dyes.

Adsorption of dyes from industrial wastewater

The industrial dye wastewater contained a direct dye and a pigment dye, which are anionic dyes used for fabric dyeing. The sample containing the direct dye had an initial basic pH with high conductivity (Table S1). After treatment with the composite, the pH was closer to neutral with a reduction of conductivity. As direct dyes are usually anionic, it can be assumed that the polymer composite would also remove other anionic dyes. Similar observations were also obtained with the pigment dye wastewater samples.

In the UV–visible spectrum, the maximum absorption was observed at 620 nm wavelength for the direct dye, and 520 nm for the pigment dye. When the dye samples were shaken with the kaolin–chitosan adsorbent for 6.0 h, the absorbance at 520 nm and 620 nm were significantly reduced (Fig. 8). These findings suggest that the synthesized

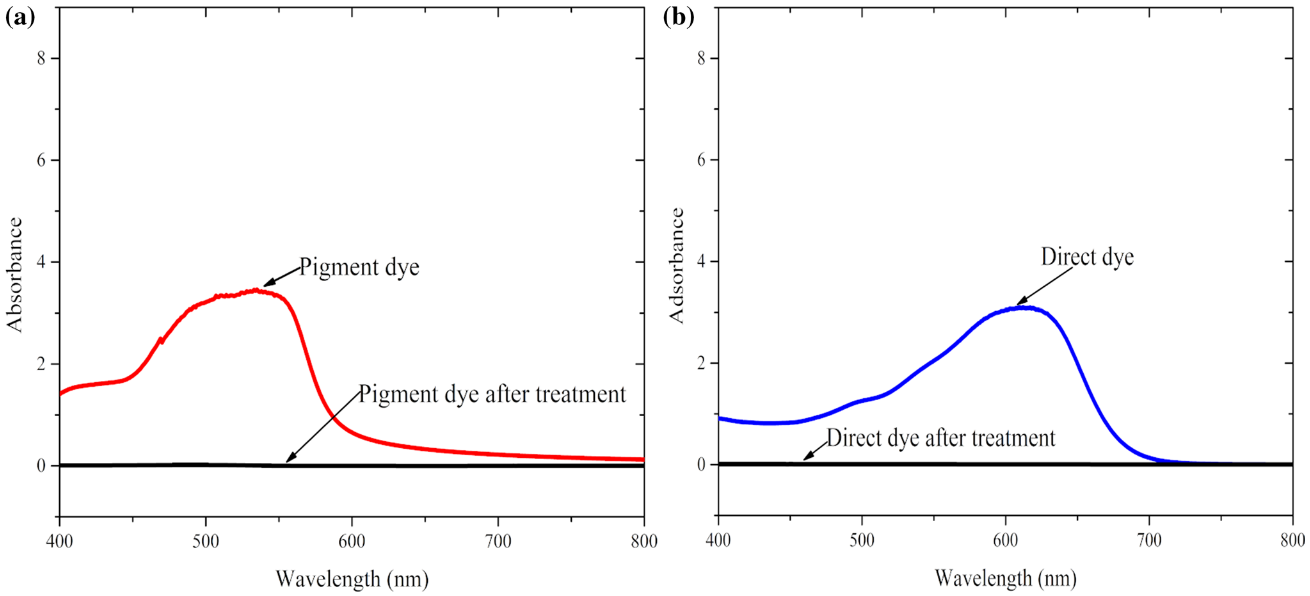

Fig. 8 Spectral scans of (**a**) pigment dye, (—) and (**b**) direct dye (—) and after treatment (—)

Table 1 Kinetics parameters for adsorption of fuchsine and methylene blue on kaolin–chitosan composite ($C_i = 5.0$ mg/L, adsorbent = 0.2 g, pH = 5.0, $T = 27$ °C, shaking speed 100 rpm, $n = 3$,)

Adsorbate	Biomass	$q_{e(exp)}$	Pseudo-first-order			Pseudo-second-order		
			k_1	q_e	R^2	k_2	q_e	R^2
Fuchsine	0.05	4.80	0.15	4.61	0.993	0.11	4.71	0.998
	0.10	3.09	0.18	3.01	0.996	0.27	3.05	0.997
	0.20	2.13	0.09	2.03	0.959	0.08	2.14	0.986
Methylene blue	0.05	6.32	0.041	5.49	0.841	0.008	6.09	0.921
	0.10	4.39	0.040	3.59	0.850	0.011	4.02	0.921
	0.20	2.09	0.023	1.96	0.976	0.013	2.23	0.997

See text for abbreviations

composite could be used to treat direct dyes, pigment dyes, and basic dyes.

Adsorption mechanism study

Kinetics of the Adsorption Process

Kinetics of the adsorption process was determined using pseudo-first-order and pseudo-second-order kinetics. The data estimated from the kinetics models can be used to identify the adsorption mechanism, which may be a mass transfer or a chemical reaction (Wu et al. 2001). Nonlinear forms of the pseudo-first-order and pseudo-second-order kinetics models are shown in Eqs. (2) and (3), respectively.

$$q_t = q_e\left(1 - \exp^{-k_1 t}\right) \tag{2}$$

$$q_t = \frac{k_2 q_e^2 t}{1 + k_2 q_e t} \tag{3}$$

where q_e and q_t is the adsorbed amount of dye (mg/g dry adsorbent) at equilibrium and at time t, respectively. The pseudo-first-order rate constant is k_1 (min^{-1}) and the pseudo-second-order rate constant is k_2 (g/mg min).

The amount of pollutant adsorbed onto the adsorbent was calculated using $q = \left(C_i - C_f\right)V/M$ where C_i is the initial dye concentration, C_f is the residual dye concentration in mg/L, M is the amount of adsorbent used in g and V is the volume of adsorbate used in L (Kumar 2006).

It was found that the pseudo-first- and pseudo-second-order kinetics agreed well with kinetics data for fuchsine adsorption on kaolin–chitosan composite with $R^2 > 0.95$. Therefore, maximum adsorption at the equilibrium time (q_e) obtained experimentally was compared with the value estimated using each model. The q_e value calculated for the pseudo-second-order kinetics model was closer to the experimental q_e value than that for the first-order kinetics model (Table 1). From this finding, it is reasonable to say the adsorption of both dyes follows the pseudo-second-order kinetics.

Similar behavior was observed for methylene blue adsorption to kaolin–chitosan composite. However, higher R^2 values were reported for the pseudo-second-order kinetics model (Table 1). From this, it is suggested that fuchsine and methylene blue adsorptions on kaolin–chitosan composite follow pseudo-second-order kinetics.

Diffusion models

Adsorption of dyes follows three main steps before it is immobilized on the adsorbent surface: (1) diffusion of the adsorbate from the bulk phase (solution) to the external surface of the adsorbent (film diffusion), (2) diffusion of adsorbate into the adsorption sites (intra-particle diffusion), and (3) attachment of the adsorbate onto adsorption sites

Table 2 Parameters of intra-particle diffusion model for fuchsine and methylene blue adsorption onto kaolin–chitosan composite ($C_i = 5.0$ mg/L, adsorbent = 0.2 g, pH = 5.0, $T = 27$ °C, shaking speed 100 rpm, $n = 3$,)

Biomass	Stage	Fuchsine			Methylene blue		
		Intercept	k_{int}	R^2	Intercept	k_{int}	R^2
0.05	Overall	4.09	0.04	0.919	1.75	0.26	0.920
	Initial				−0.59	0.94	0.887
	Final				1.92	0.24	0.989
0.10	Overall	2.82	0.01	0.80	1.14	0.16	0.902
	Initial				−0.42	0.59	0.974
	Final				1.68	0.11	0.988
0.20	Overall	1.51	0.04	0.916	0.37	0.10	0.922
	Initial				−0.11	0.21	0.990
	Final				0.84	0.07	0.965

See text for abbreviations

Table 3 Parameters of the isotherm models for fuchsine and methylene blue adsorption onto kaolin–chitosan composite (adsorbent = 0.2 g, pH = 5.0, $T = 27$ °C, shaking speed 100 rpm, $n = 3$,)

Adsorbate	Model	k	q_0	$n/g/B_s$	E	C_s	R^2
Fuchsine	Langmuir	1.19	7.11				0.991
	Freundlich	3.33		2.21			0.965
	Dubinin–Radushkevich	6.58×10^{-03}	6.93		8.72	15.16	0.993
	Langmuir–Freundlich	0.87	8.00	0.86			0.991
Methylene blue	Langmuir	1.46	4.70				0.807
	Freundlich	2.69		3.37			0.981
	Dubinin–Radushkevich	0.02	150.49		4.99	1.18E^{+12}	0.927
	Langmuir–Freundlich	5.14×10^{-07}	210.93	0.3			0.972

See text for abbreviations

(interaction). Liquid film diffusion and intra-particle diffusion are given by Eqs. (4) and (5), respectively (Plazinski 2010; Dissanayake et al. 2016).

$$q_t = k_{\text{int}} t^{0.5} \tag{4}$$

$$\ln\left(1 - \frac{q_t}{q_e}\right) = -R^1 t \tag{5}$$

where k_{int} and R^1 are the intra-particle diffusion constant, liquid film diffusion constant (min^{-1}), respectively and R^1 is given by

$$R^1 = \frac{3D_e^1}{r_0 \Delta r_0 k^1}$$

where $D_e{}^1$, r_0, Δr_0, and k^1 denotes the diffusion coefficient of effective liquid film (cm^2/min), adsorbent particle radius (cm), liquid film thickness (cm), and R^1 is the equilibrium constant of adsorption, respectively.

A linear relationship with an intercept of zero for the plot of q_t versus $t^{0.5}$ shows intra-particle diffusion determined the adsorption rate. If the straight line does not pass through the origin, it is assumed that there are rate limiting steps other than intra-particle diffusion. Parameters of the intra-particle diffusion model is listed in Table 2.

The fuchsine adsorption followed the intra-particle diffusion model with nonzero intercept, indicates that there are other rate limiting steps involved in the process (supplementary material Fig. S1). However, methylene blue adsorption follows the intra-particle model with two steps—a rapid initial step with an intercept close to zero, and a slow later stage with nonzero intercept. This, suggests that the methylene blue adsorption is initially controlled by intra-particle diffusion, and later other rate limiting factors are also involved in determining the adsorption rate.

The adsorption system follows the liquid film diffusion model when the ln $(1 - q_t/q_e)$ vs. t plot is linear and the gradient $(-R^1)$ is negative (Supplementary Material Fig. S2 Table S2). For both adsorbates, the liquid film diffusion model is also involved in rate limiting. However, methylene blue adsorption showed three separate steps for the plot: (1) rapid initial step, (2) slow middle step, and (3) rapid final step. This is mainly due to the concentration gradient between the bulk solution and the adsorbent surface.

Adsorption isotherms of the process

The adsorbate–adsorbent interaction of fuchsine and methylene blue, with the kaolin–chitosan composite adsorbent, was investigated using two parameter isotherms (Langmuir, Freundlich and Dubinin–Radushkevich), and three parameter isotherms (Langmuir–Freundlich combined isotherm). Plot of q_e vs C_e was used to determine the value of each parameter (Dada et al. 2012; Dissanayake et al. 2016).

The Langmuir isotherm model (valid for monolayer adsorption) was determined from Eq. 6. The adsorption intensity was calculated using Eq. 7.

$$q_e = \frac{q_0 b C_e}{1 + bC_e} \tag{6}$$

$$R_L = 1/(1 + bC_i) \tag{7}$$

where the absorbed amount of dye at equilibrium and maximum adsorption capacity are denoted by q_e and q_0 (mg/g), respectively, The Langmuir isotherm constant is denoted by b, and residual adsorbate concentration by C_e (mg/L) at equilibrium. (Krishna Prasad and Srivastava 2009).

Four probabilities are possible for the R_L values: (1) $0 < R_L < 1$, favorable adsorption; (2) $R_L > 1$, unfavorable adsorption; (3) $R_L = 1$, linear adsorption; and (4) $R_L = 0$, irreversible adsorption (Dissanayake et al. 2016).

The fuchsine adsorption onto the composite adsorbent showed a better agreement with the Langmuir model with a high R^2 of 0.991 (Table 3). However, methylene blue adsorption does not follow the Langmuir model (Table 3, Supplementary Material Fig. S3). Therefore, it is postulated that fuchsine interacts with the adsorbent chemically and the methylene blue molecule interaction may not be chemical (Padmesh et al. 2006). The R_L obtained for fuchsine adsorption onto the composite was between 0.05 and 0.43, which falls into the favorable adsorption process. Even though methylene blue adsorption did not follow the Langmuir isotherm, R_L value was between 0.33 and 0.89, which indicated that the adsorption is favorable.

Multilayer adsorption of adsorbate on the heterogeneous adsorbent surface is described by the Freundlich isotherm, is given by Eq. 8,

$$q_e = k_f C_e^{1/n} \tag{8}$$

where adsorption capacity and the adsorption intensity denoted by k_f and n, respectively (Liu et al. 2010; Dissanayake et al. 2016).

The lowest R^2 of 0.965 (Table 3, Supplementary material Fig. S3) was reported for the Freundlich isotherm for fuchsine adsorption on the composite surface. However, the highest R^2 of 0.981 (Table 3) for methylene blue adsorption was reported for the Freundlich isotherm. The $1/n$ values obtained for the fuchsine and methylene adsorption were 0.45 and 0.29, respectively; hence, the surface is energetically heterogeneous (Aravindhan et al. 2007).

The mean free energy distribution is used to express the Dubinin–Radushkevich (D–R) isotherm model and the model assumes chemisorption onto a heterogeneous surface. The D–R model is described by Eq. 9:

$$q_e = q_0 \exp\left\{-\left[\frac{RT\ln(C_s/C_e)}{E}\right]^2\right\} \tag{9}$$

where R, and T are the universal gas constant and absolute temperature (K), respectively. The saturation concentration is denoted by C_s. The mean free energy (E) equation $\left[E = [\frac{1}{\sqrt{2\beta}}]\right]$ was used to determine the Dubinin–Radushkevich constant β (mol^2/J^2) (Nguyen and Do 2001).

Adsorption of both fuchsine and methylene blue on the composite surface showed a better agreement with experimental data, according to R^2 values. The mean free energy for fuchsine and methylene blue adsorption were 8.72 kJ/mol and 4.99 kJ/mol, respectively (Table 3, Supplementary Material Fig. S3). These observations confirm that the adsorption of fuchsine is chemisorption onto a heterogeneous surface, while that of methylene blue is physisorption (Oyelude et al. 2015).

Equation 10 describes the Langmuir and Freundlich (L–F) combined isotherm model:

$$q_e = \frac{q_0 (k_a C_e)^n}{(k_a C_e)^n + 1} \tag{10}$$

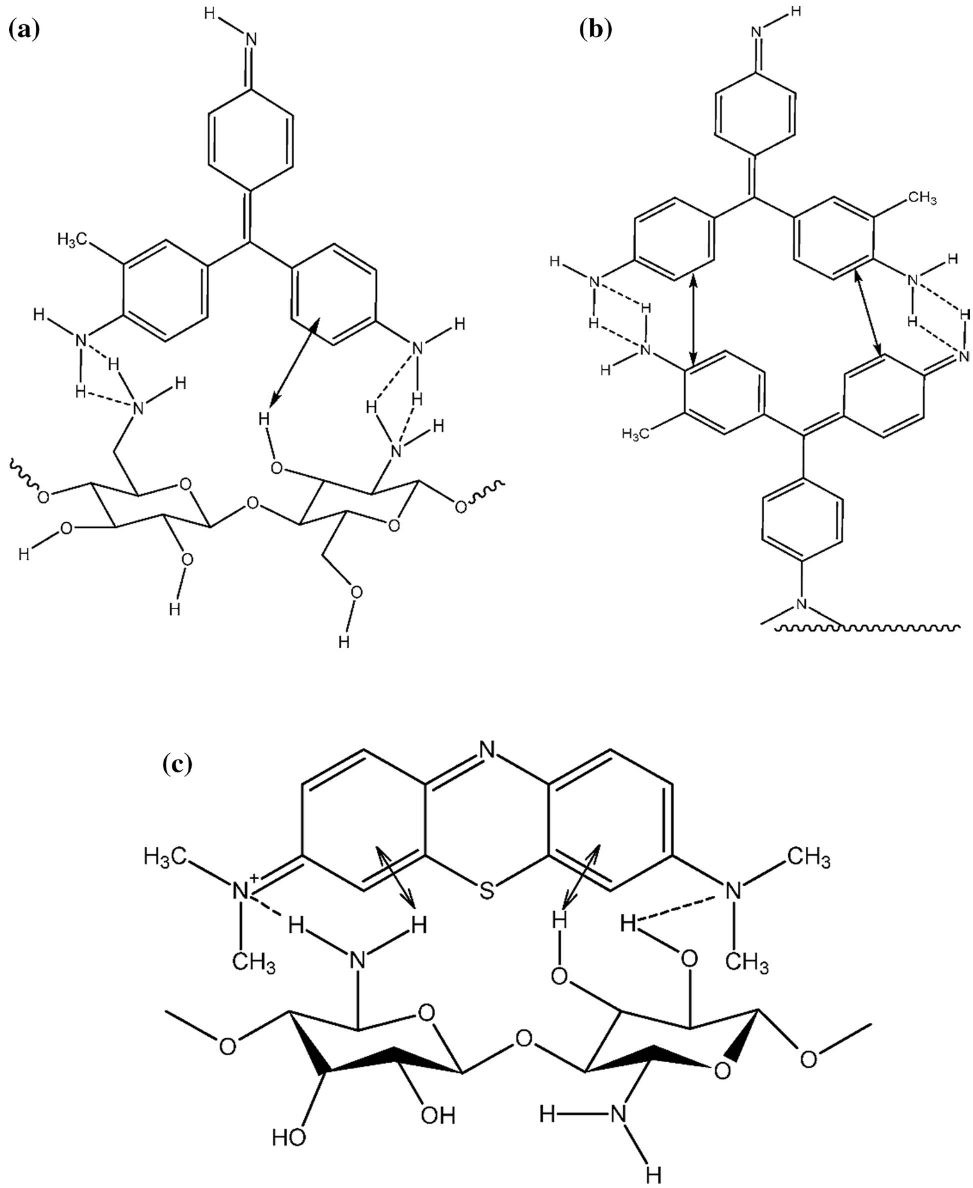

Scheme 1 Schematic diagram for the proposed (**a**) interactions between chitosan and the fuchsine dye (**b**) formation of multilayers (**c**) interactions between chitosan and methylene blue (⟷ π electron interactions, hydrogen bonds)

where the affinity constant and heterogeneity index is denoted by k_a (L/mg) and n, respectively (Jeppu and Clement 2012).

From the results shown in Table 3, the L–F combined model is appropriate to describe the nature of the adsorption where it showed relatively high R^2 value. From the isotherm study, it is possible to conclude that fuchsine adsorption on the heterogeneous polymer composite surface is a chemical process, while it is a physisorption process for methylene blue (Turiel et al. 2003).

Mechanism of dye adsorption

The isotherm study shows that dye molecules interact with the adsorbent surface through physical and chemical interactions. Initially, amine groups of fuchsine dye form interactions with the functional groups on the adsorbent surface. These functional groups are Si–OH, R–OH, and R–NH_2. The interactions could be hydrogen bonds, charged interactions, and acid base interactions shown in Scheme 1a (Brown et al. 1980; Spencer et al. 1985). The high concentration of

Table 4 Comparison of fuchsine and methylene blue adsorption by adsorbent

Adsorbate	Adsorbent	Removal %	References
Fuchsine	Cellulose modified with maleic anhydride	88.10	(Zhou et al. 2012)
	Magnetic NaY zeolite	98.1	(Shirani et al. 2014)
	Phosphonate metal–organic frameworks	65	(Nistor et al. 2020)
	Cobalt-doped alumina hybrids	68	(Parveen and Rafique 2018)
	Asplenium nidus biosorbent	88	(Dissanayake et al. 2016)
	Chicken bones activated carbon	93.63	(Cortes et al. 2019)
	Cellulose-based multicarboxyl adsorbent	85	(Zhou et al. 2013)
	Activated carbons from lignin	57	(Cotoruelo et al. 2011)
	Kaolin–chitosan composite	93	Present study
Methylene blue	Activated lignin–chitosan extruded blends	87.69	(Albadarin et al. 2017)
	Bituminous coal	96.5	(Huang et al. 2019)
	Sodium vinyl sulfonate-co-2-acrylamido-2-methylpropane sulfonic acid sodium salt-magnetite cryogel	99.8	(Al-Hussain et al. 2018)
	Ca^{2+}-based metal–organic framework	80–88	(Liu et al. 2020)
	Bone char	42–45	(Khoo et al. 2012)
	Biogenic selenium nanoparticles	49	(Xia et al. 2018)
	chitosan/polyacrylamide/graphene oxide	90.18	(Wang et al. 2020)
	Thiourea-modified Poly(acrylonitrile-co-acrylic acid)	90–95	(Adeyi et al. 2019)
	Kaolin–chitosan composite	95	Present study

the dye could cover the adsorbant surface thus preventing new dye molecules to interact with the adsorbent (Zhang et al. 2005). However, the dye molecules that have already formed interactions can form π–π electron interactions with new dye molecules due to the presence of phenyl groups in the dye (Jain et al. 2009; Dissanayake et al. 2016). Therefore, multilayers of fuchsine would form due to the hydrogen bond formation and π–π electron interactions between dyes (Scheme 1b). The methylene blue molecules are arranged on the adsorbent surface by forming H–π, hydrogen bonds and charge interactions (Scheme 1c). This may be the reason for the higher equilibrium time needed for adsorption of methylene blue than for fuchsine.

Significance of the study

Adsorption of fuchsine and methylene blue by kaolin–chitosan composite was compared with that by other adsorbents reported in the recent literature (Table 4). Some adsorbents reported lower adsorption of 57–68% for fuchsine (Cotoruelo et al. 2011; Nistor et al. 2020) and 42–49% for methylene blue (Khoo et al. 2012; Xia et al. 2018); in this study, the kaolin–chitosan composite dose of 0.20 g adsorbed > 90%. A similar dose of kaolin–chitosan composite considerably removed direct and pigment dyes, from an industrial sample, showing potential for its use in remediating dye-containing wastewater. Further, preparation of the kaolin–chitosan composite adsorbent does not require expert knowledge and is a simple process.

Conclusion

This kaolin–chitosan composite prepared by the solgel method, having demonstrated an attractive surface area, leads to excellent adsorption capacity toward fuchsine and methylene blue dyes. The strength of interaction of these two dyes with the composite upon adsorption is confirmed through peak shifts in Fourier transform infrared spectra and surface changes in scanning electron microscopic images. Adsorption of both dyes follows the pseudo-second-order kinetics, and further, the adsorption process is governed by intra-particle diffusion and liquid film diffusion. The adsorption of fuchsine adequately follows the Langmuir–Freundlich isotherm model and that of methylene blue follows the Freundlich isotherm model. Therefore, it is evident that fuchsine adsorption is a combination of chemisorption and physisorption, while methylene blue adsorption is solely physisorption. The composite is also capable of removing negatively charged dyes, such as pigment dyes and direct dyes, since the adsorption surface is positively charged even at pH 7. Therefore, it is concluded that the kaolin–chitosan composite adsorbent be used for efficient treatment of anionic textile dye-contaminated wastewater. More importantly, the composite dose of 0.20 g is able to adsorb pigment dyes and direct dyes present in a sample of industrial wastewater within 6.0 h of agitation. Having demonstrated this application, the next logical step of this research would be to extend the findings of adsorption equilibrium and kinetics toward dynamic studies and prototype system measurements in real-time situations.

Supplementary Information The online version contains supplementary material available at https://doi.org/10.1007/s13762-021-03711-6.

Acknowledgements The authors express their gratitude to Shirani Perera and R. B. Hapukotuwa of the National Institute of Fundamental Studies, Sri Lanka, for providing assistance in the laboratory. Valuable feedback from Tim Schaefer, Institute for Physical Chemistry, Faculty of Chemistry, Georg-August University, Goettingen, Germany during the preparation of this manuscript is highly appreciated. Financial support from the National Research Council, Sri Lanka (Grant No: 13-087) is highly acknowledged.

Author contributions Conceptualization: READ, SSI, NP and MCM-Iqbal; data curation: READ and IMP; funding acquisition: MCMI; methodology: READ and IMP; supervision: SSI, NP and MCMI; writing—original draft: READ; writing—review and editing: NP, SSI and MCMI.

Funding National Research Council of Sri Lanka Grant No: 13-087.

Data availability Data will be available upon a reasonable request.

Declarations

Conflict of interest Authors declare no conflict of interest.

References

Adeyi AA, Jamil SNAM, Abdullah LC et al (2019) Adsorptive removal of methylene blue from aquatic environments using thiourea-modified poly (Acrylonitrile-co-Acrylic Acid). Materials (Basel) 12:1734. https://doi.org/10.3390/ma12111734

Albadarin AB, Collins MN, Naushad M et al (2017) Activated lignin-chitosan extruded blends for efficient adsorption of methylene blue. Chem Eng J 307:264–272. https://doi.org/10.1016/j.cej.2016.08.089

Alexandre M, Dubois P (2000) Polymer-layered silicate nanocomposites: Preparation, properties and uses of a new class of materials. Mater Sci Eng R Rep 28:1–63. https://doi.org/10.1016/S0927-796X(00)00012-7

Al-Hussain S, Atta A, Al-Lohedan H et al (2018) Application of new sodium vinyl Sulfonate–co-2-Acrylamido-2-me[thylpropane sulfonic acid sodium salt-magnetite cryogel nanocomposites for fast methylene blue removal from industrial waste water. Nanomaterials 8:878. https://doi.org/10.3390/nano8110878

Amer MW, Khalili FI, Awwad AM (2010) A dsorption of lead, zinc and cadmium ions on polyphosphate-modified kaolinite clay. J Environ Chem Ecotoxicol 2:001–008

Aravindhan R, Rao JR, Nair BU (2007) Removal of basic yellow dye from aqueous solution by sorption on green alga Caulerpa scalpelliformis. J Hazard Mater 142:68–76. https://doi.org/10.1016/j.jhazmat.2006.07.058

Asgher M, Arshad S, Qamar SA, Khalid N (2020) Improved biosurfactant production from Aspergillus niger through chemical mutagenesis: characterization and RSM optimization. SN Appl Sci 2:1–11. https://doi.org/10.1007/s42452-020-2783-3

Brown NMD, Floyd RB, Nelson WJ, Walmsley DG (1980) Inelastic electron tunnelling spectroscopy of selected alcohols and amines on plasma-grown aluminium oxide. J Chem Soc Faraday Trans 1 Phys Chem Condens Phases 76:2335–2346. https://doi.org/10.1039/F19807602335

Bulut Y, Aydın H (2006) A kinetics and thermodynamics study of methylene blue adsorption on wheat shells. Desalination 194:259–267. https://doi.org/10.1016/j.desal.2005.10.032

Cestari AR, Vieira EFS, Tavares AMG, Bruns RE (2008) The removal of the indigo carmine dye from aqueous solutions using cross-linked chitosan-Evaluation of adsorption thermodynamics using a full factorial design. J Hazard Mater 153:566–574. https://doi.org/10.1016/j.jhazmat.2007.08.092

Chang MY, Juang RS (2004) Adsorption of tannic acid, humic acid, and dyes from water using the composite of chitosan and activated clay. J Colloid Interface Sci 278:18–25. https://doi.org/10.1016/j.jcis.2004.05.029

Chathuranga PKD, Dissanayake DMREA, Priyantha N et al (2014) Biosorption and desorption of lead(II) by *Hydrilla verticillata*. Bioremediat J 18:192–203. https://doi.org/10.1080/10889868.2014.910492

Chequer F, de Oliveira GAR, Anastacio Ferraz ER, et al (2013) Textile dyes: dyeing process and environmental impact. In: Günay M (ed.), Eco-friendly textile dyeing and finishing. InTech, pp 151–176

Cortes LN, Druzian SP, Mantelli Streit AF et al (2019) Preparation of carbonaceous materials from pyrolysis of chicken bones and its application for fuchsine adsorption. Environ Sci Pollut Res 26:28574–28583. https://doi.org/10.1007/s11356-018-3679-2

Cotoruelo LM, Marques MD, Rodriguez-Mirasol J et al (2011) Cationic dyes removal by multilayer adsorption on activated carbons from lignin. J Porous Mater 18:693–702. https://doi.org/10.1007/s10934-010-9428-7

Dada AO, Olalekan AP, Olatunya AM, Dada O (2012) Langmuir, freundlich, temkin and dubinin: radushkevich isotherms studies of equilibrium sorption of Zn2+ unto phosphoric acid modified rice husk. IOSR J Appl Chem 3:38–45. https://doi.org/10.9790/5736-0313845

Dissanayake DMREA, Wijesinghe WMKEH, Iqbal SS et al (2016) Fuchsine biosorption using Asplenium nidus biosorbent-a mechanism using kinetic and isotherm data. RSC Adv 6:98682–98692. https://doi.org/10.1039/C6RA19011A

Fein JB, Boily JF, Yee N et al (2005) Potentiometric titrations of *Bacillus subtilis* cells to low pH and a comparison of modeling approaches. Geochim Cosmochim Acta 69:1123–1132. https://doi.org/10.1016/j.gca.2004.07.033

Guo Y, Yang S, Fu W et al (2003) Adsorption of malachite green on micro-and mesoporous rice husk-based active carbon. Dye Pigment 56:219–229

Gupta VK, Mittal A, Gajbe V, Mittal J (2008) Adsorption of basic fuchsin using waste materials: bottom ash and deoiled soya—as adsorbents. J Colloid Interface Sci 319:30–39

Huang B, Zhao R, Xu H et al (2019) Adsorption of methylene blue on bituminous coal: adsorption mechanism and molecular simulation. ACS Omega 4:14032–14039. https://doi.org/10.1021/acsomega.9b01812

Iqbal HMN, Rasheed T, Bilal M (2018) Design and processing aspects of polymer and composite materials. Green and sustainable advanced materials. Wiley, Hoboken, NJ, USA, pp 155–189

Islam M, Masum S, Rahman MM et al (2011) Preparation of chitosan from shrimp shell and investigation of its properties. Int J Basic Appl Sci 77–80

Jain A, Ramanathan V, Sankararamakrishnan R (2009) Lone pair π interactions between water oxygens and aromatic residues: quantum chemical studies based on high-resolution protein structures and model compounds. Protein Sci 18:595–605. https://doi.org/10.1002/pro.67

Jeppu GP, Clement TP (2012) A modified Langmuir-Freundlich isotherm model for simulating pH-dependent adsorption effects. J Contam Hydrol 129–130:46–53. https://doi.org/10.1016/j.jconhyd.2011.12.001

Jiang L, Zhang J (2017) Biodegradable and biobased polymers. In: Applied plastics engineering handbook: processing, materials, and applications: Second Edition. Elsevier Inc., pp 127–143

Kalemtas A (2019) Effect of the sintering temperature on the fabrication of alumina beads. Mater Sci Res India 16:125–135. https://doi.org/10.13005/msri/160206

Karaca S, Gürses A, Açikyildiz M, Ejder (Korucu) M (2008) Adsorption of cationic dye from aqueous solutions by activated carbon. Microporous Mesoporous Mater 115:376–382. https://doi.org/10.1016/j.micromeso.2008.02.008

Khoo EC, Ong ST, Ha ST (2012) Removal of basic dyes from aqueous environment in single and binary systems by sugarcane bagasse in a fixed-bed column. Desalin Water Treat 37:215–222. https://doi.org/10.5004/dwt.2012.2219

Krishna Prasad R, Srivastava SN (2009) Sorption of distillery spent wash onto fly ash: kinetics and mass transfer studies. Chem Eng J 146:90–97. https://doi.org/10.1016/j.cej.2008.05.021

Kumar KV (2006) Linear and non-linear regression analysis for the sorption kinetics of methylene blue onto activated carbon. J Hazard Mater 137:1538–1544. https://doi.org/10.1016/j.jhazmat.2006.04.036

Liu Z, Xia X, Li W et al (2020) In situ growth of ca -based metal–organic framework on CaSiO /ABS/TPU 3D skeleton for methylene blue removal. Materials (Basel) 13:4403. https://doi.org/10.3390/ma13194403

Liu Q-S, Zheng T, Wang P et al (2010) Adsorption isotherm, kinetic and mechanism studies of some substituted phenols on activated carbon fibers. Chem Eng J 157:348–356. https://doi.org/10.1016/j.cej.2009.11.013

Meroufel B, Benali O, Benyahia M et al (2013) Adsorptive removal of anionic dye from aqueous solutions by Algerian kaolin: characteristics, isotherm, kinetic and thermodynamic studies. J Mater Environ Sci 4:482–491

Mgbemena CO, Ibekwe NO, Sukumar R, Menon ARR (2013) Characterization of kaolin intercalates of oleochemicals derived from rubber seed (*Hevea brasiliensis*) and tea seed (*Camelia sinensis*) oils. J King Saud Univ 25:149–155

Mittal V (2009) Polymer layered silicate nanocomposites: a review. Materials (basel) 2:992–1057. https://doi.org/10.3390/ma2030992

Monvisade P, Siriphannon P (2009) Chitosan intercalated montmorillonite: preparation, characterization and cationic dye adsorption. Appl Clay Sci 42:427–431. https://doi.org/10.1016/j.clay.2008.04.013

Mota JA, Chagas RA, Vieira EFS, Cestari AR (2012) Synthesis and characterization of a novel fish scale-immobilized chitosan adsorbent-preliminary features of dichlorophenol sorption by solution calorimetry. J Hazard Mater 229–230:346–353. https://doi.org/10.1016/j.jhazmat.2012.06.010

Nesic AR, Velickovic SJ, Antonovic DG (2012) Characterization of chitosan/montmorillonite membranes as adsorbents for Bezactiv Orange V-3R dye. J Hazard Mater 209–210:256–263. https://doi.org/10.1016/j.jhazmat.2012.01.020

Nguyen C, Do DD (2001) The Dubinin-Radushkevich equation and the underlying microscopic adsorption description. Carbon N Y 39:1327–1336. https://doi.org/10.1016/S0008-6223(00)00265-7

Nistor MA, Muntean SG, Maranescu B, Visa A (2020) Phosphonate metal-organic frameworks used as dye removal materials from wastewaters. Appl Organomet Chem. https://doi.org/10.1002/aoc.5939

Oyelude EO, Frimpong F, Dawson D (2015) Studies on the removal of basic fuchsin dye from aqueous solution by HCl treated malted sorghum mash. J Mater Environ Sci 6:1126–1136

Padmesh TVN, Vijayaraghavan K, Sekaran G, Velan M (2006) Application of two- and three-parameter isotherm models: Biosorption of Acid Red 88 onto *Azolla microphylla*. Bioremediat J 10:37–44. https://doi.org/10.1080/10889860600842746

Parveen K, Rafique U (2018) Development of cobalt-doped alumina hybrids for adsorption of textile effluents. Adsorpt Sci Technol 36:182–197. https://doi.org/10.1177/0263617416687563

Paul DR, Robeson LM (2008) Polymer nanotechnology: nanocomposites. Polymer 49:3187–3204. https://doi.org/10.1016/j.polymer.2008.04.017

Pavlidou S, Papaspyrides CD (2008) A review on polymer: layered silicate nanocomposites. Prog Polym Sci 33:1119–1198. https://doi.org/10.1016/j.progpolymsci.2008.07.008

Plazinski W (2010) Applicability of the film-diffusion model for description of the adsorption kinetics at the solid/solution interfaces. Appl Surf Sci 256:5157–5163. https://doi.org/10.1016/j.apsusc.2009.12.083

Qamar SA, Ashiq M, Jahangeer M et al (2020) Chitosan-based hybrid materials as adsorbents for textile dyes: a review. Case Stud Chem Environ Eng 2:100021. https://doi.org/10.1016/j.cscee.2020.100021

Rekik SB, Gassara S, Bouaziz J et al (2017) Development and characterization of porous membranes based on kaolin/chitosan composite. Appl Clay Sci 143:1–9. https://doi.org/10.1016/j.clay.2017.03.008

Rosales E, Meijide J, Pazos M, Sanromán MA (2017) Challenges and recent advances in biochar as low-cost biosorbent: from batch assays to continuous-flow systems. Bioresour Technol 246:176–192. https://doi.org/10.1016/j.biortech.2017.06.084

Saikia BJ, Parthasarathy G (2010) Fourier transform infrared spectroscopic characterization of kaolinite from Assam and Meghalaya. Northeastern India J Mod Phys 1:206

Shirani M, Semnani A, Haddadi H, Habibollahi S (2014) Optimization of simultaneous removal of methylene blue, crystal violet, and fuchsine from aqueous solutions by magnetic nay zeolite composite. Water Air Soil Pollut 225:1–15. https://doi.org/10.1007/s11270-014-2054-2

Spencer JN, Wolbach WS, Hovick JW et al (1985) Hydrogen bonding by alcohols and amines. J Solut Chem 14:805–814. https://doi.org/10.1007/BF00646002

Tironi A, Trezza MA, Irassar EF, Scian AN (2012) Thermal treatment of kaolin: effect on the pozzolanic activity. Procedia Mater Sci 1:343–350

Turiel E, Perez-Conde C, Martin-Esteban A (2003) Assessment of the cross-reactivity and binding sites characterisation of a propazine-imprinted polymer using the Langmuir-Freundlich isotherm. Analyst 128:137–141. https://doi.org/10.1039/b210712k

Vakili M, Rafatullah M, Salamatinia B et al (2014) Application of chitosan and its derivatives as adsorbents for dye removal from water and wastewater: a review. Carbohydr Polym 113:115–130

Volesky B (2003) The mechanism of metal biosorption. In: Sorption and biosorption. BV sorbex Inc, pp 41–46

Wan Ngah WS, Teong LC, Hanafiah MAKMKM (2011) Adsorption of dyes and heavy metal ions by chitosan composites: A review. Carbohydr Polym 83:1446–1456. https://doi.org/10.1016/j.carbpol.2010.11.004

Wang Z, Zhang G, Li Y (2020) Preparation of Chitosan/Polyacrylamide/Graphene oxide composite membranes and study of their methylene blue adsorption properties. Materials (Basel) 13:4407. https://doi.org/10.3390/ma13194407

Wu F-C, Tseng R-L, Juang R-S (2001) Kinetic modeling of liquid-phase adsorption of reactive dyes and metal ions on chitosan. Water Res 35:613–618

Xia X, Zhou Z, Wu S et al (2018) Adsorption removal of multiple dyes using biogenic selenium nanoparticles from an escherichia coli strain overexpressed selenite reductase CsrF. Nanomaterials 8:234. https://doi.org/10.3390/nano8040234

Xie H, Jia Z, Huang J, Zhang C (2011) Study on the preparation of superabsorbent composite of chitosan-g-poly (acrylic acid)/kaolin by in-situ polymerization. Int J Chem 3:69–74. https://doi.org/10.5539/ijc.v3n3p69

Zhang W-MM, Chen J-LL, Pan B-CC, Zhang Q-XX (2005) Competitive and cooperative adsorption behaviors of phenol and aniline onto nonpolar macroreticular adsorbents. J Environ Sci 17:529–534. https://doi.org/10.1260/026361705776316541

Zhou L, Jin J, Liu Z et al (2011) Adsorption of acid dyes from aqueous solutions by the ethylenediamine-modified magnetic chitosan nanoparticles. J Hazard Mater 185:1045–1052. https://doi.org/10.1016/j.jhazmat.2010.10.012

Zhou Y, Jin Q, Hu X et al (2012) Heavy metal ions and organic dyes removal from water by cellulose modified with maleic anhydride. J Mater Sci 47:5019–5029. https://doi.org/10.1007/s10853-012-6378-2

Zhou Y, Zhang M, Hu X et al (2013) Adsorption of cationic dyes on a cellulose-based multicarboxyl adsorbent. J Chem Eng Data 58:413–421. https://doi.org/10.1021/je301140c

Zhu HY, Jiang R, Xiao L (2010) Adsorption of an anionic azo dye by chitosan/kaolin/γ-Fe_2O_3 composites. Appl Clay Sci 48:522–526. https://doi.org/10.1016/j.clay.2010.02.003

Zhu HY, Jiang R, Fu YQ et al (2011) Preparation, characterization and dye adsorption properties of γ-Fe2O3/SiO2/chitosan composite. Appl Surf Sci 258:1337–1344. https://doi.org/10.1016/J.APSUSC.2011.09.045